Wasit Journal for Pure Science



Journal Homepage: https://wjps.uowasit.edu.iq/index.php/wjps/index
e-ISSN: 2790-5241 p-ISSN: 2790-5233

Numerical Simulation of a Nonlinear Predator-Prey System with Robin Boundary Conditions

Huda R. Al-Maliky¹, Ghassan A. Al-Juaifri²

^{1,2}Department of Mathematics, Faculty of Computer Science and Mathematics, University of Kufa, IRAQ.

*Corresponding Author: Huda R. Al-Maliky

DOI: https://doi.org/10.31185/wjps.776

Received 10 February 2025; Accepted 21 April 2025; Available online 30 September 2025

ABSTRACT: This study investigates a nonlinear predator—prey system modeled by reaction—diffusion equations in a convex, open domain with Robin boundary conditions. The system is discretized and solved using the Finite Element Method (FEM), providing an effective framework to capture the spatiotemporal dynamics of predator—prey interactions. An error analysis is performed to assess the accuracy of the numerical solutions relative to the exact continuous solution. The results demonstrate the reliability and efficiency of the proposed numerical scheme, highlighting its capability to handle the complexities associated with Robin boundary conditions.

Keywords: predator-prey system, Robin boundary, fully-discrete approximation, error estimate.



©2025 THIS IS AN OPEN ACCESS ARTICLE UNDER THE CC BY LICENSE

1. INTRODUCTION

The importance of reaction—diffusion systems with Robin boundary conditions can be attributed to several factors. Despite extensive research on reaction—diffusion systems with Dirichlet and Neumann boundary conditions, comparatively little work has been conducted on systems with Robin boundary conditions [21]. From an application perspective, the Dirichlet condition is often employed as a simple approximation to a more realistic Robin condition in systems of "oscillatory" reaction—diffusion equations. In this paper, we investigate a predator—prey system consisting of two coupled components subject to Robin boundary conditions for the reaction—diffusion equations [13]:

(H) Find {p,q}\{p,q\} {p,q} } such that

$$\frac{\partial p}{\partial t} = \Delta p + f_1(p, q),$$
 in λ_T , (1)

$$\frac{\partial q}{\partial t} = \Delta q + f_2(p, q), \qquad \text{in} \qquad \lambda_T, \tag{2}$$

$$\frac{\partial p}{\partial \nu} + \gamma p = 0, \qquad \frac{\partial q}{\partial \nu} + \gamma q = 0, \qquad \text{on} \quad \partial \lambda_T, \tag{3}$$

$$p(\cdot,0) = p_0, \qquad q(\cdot,0) = q_0, \qquad \text{in} \quad \lambda, \tag{4}$$

where, $\rho^2 = p^2 + q^2$ and $\lambda_T = \lambda \times (0,T)$, λ is an open bounded convex domain in $\mathbb{R}^d(d=1,2,3)$, with $\partial \lambda$ sufficiently smooth, $\partial \lambda_T = \partial \lambda \times (0,T)$, ν denotes the exterior unit normal to $\partial \lambda$, moreover $f_1(p,q) = (1-\rho^2)p - (\omega_1 - \omega_2\rho^2)q$, $f_2(p,q) = (\omega_1 - \omega_2\rho^2)p + (1-\rho^2)q$ and ω_1 , ω_2 and γ are positive constants. Reaction-diffusion systems on the boundary, which are systems of nonlinear parabolic partial differential equations, have been the focus of active research for many years. These systems have a wide range of applications in physics, chemistry, ecology, biology, and other disciplines. For comprehensive reviews of the theory and applications of reaction-diffusion systems, see Britton [7], Murray [18], Volpert et al. [23], Hashim and Harfash [11], and Al-Juaifri and Harfash [2].

Our assumptions throughout are as follows:

Theorem 1.1. Suppose that $p_0, q_0 \in H^1(\lambda)$, then the system (H) possesses a unique Higher regularity solution $\{p, q\}$ satisfying

$$p(.,t), q(.,t) \in L^{2}(0,T;H^{2}(\lambda)) \cap L^{\infty}(0,T;L^{4}(\lambda))$$

$$\cap L^{\infty}(0,T;H^{1}(\lambda)) \cap L^{6}(\lambda_{T}) \cap C([0,T];H^{1}(\lambda)),$$

$$\frac{\partial p(.,t)}{\partial t}, \frac{\partial q(.,t)}{\partial t} \in L^{2}(\lambda_{T}),$$
and the system (H) hold as equalities in $L^{2}(\lambda_{T})$. Moreover, the solution Continuous dependence on the initial data in

 $H^2(\lambda)$.

$$(p_0(.), q_0(.)), \mapsto (p(., t; p_0, q_0), q(., t; p_0, q_0)),$$

is continuous in $H^1(\lambda)$.

NUMERICAL ALGORITHM

At each time level, we first describe the following practical approach for solving the nonlinear algebraic system that arises from the approximated problem:

Given
$$\{P^{n,0}, Q^{n,0}\} \in S^h \times S^h$$
, then for $k \ge 1$ find $\{P^{n,k}, Q^{n,k}\} \in S^h \times S^h$ such that for all $\varpi^h \in S^h$

$$(\frac{P^{n,k}-P^{n-1}}{\Delta t}, \varpi^h)^h + (\nabla P^{n,k}, \nabla \varpi^h) + \gamma \int_{\partial \lambda} P^{n,k} \varpi^h dA$$

$$= ((1 - (\rho^{n,k-1})^2)P^{n,k}, \varpi^h)^h - ((w_1 - w_2(\rho^{n,k-1})^2)Q^{n,k-1}, \varpi^h)^h,$$
(7)

$$\frac{(Q^{n,k}-Q^{n-1})}{\Delta t}, \varpi^h)^h + (\nabla Q^{n,k}, \nabla \varpi^h) + \gamma \int_{\partial \lambda} Q^{n,k} \varpi^h dA
= ((w_1 - w_2(\rho^{n,k-1})^2)P^{n,k-1}, \varpi^h)^h + ((1 - (\rho^{n,k-1})^2)Q^{n,k-1}, \varpi^h)^h.$$
(8)

We start with $P^0 \equiv \pi^h p^0$, and $Q^0 \equiv \pi^h q^0$, and then, for $n \ge 1$, we set $P^{n,0} \equiv P^{n-1}$ and $Q^{n,0} \equiv Q^{n-1}$. From (7) and (8), a linear system, for $2 \times (J+1)^d$, d=1,2,3 linear equations, can be found by testing (7) and (8) by φ_j , j=1,2,30,..., I. Using the Gauss-Seidel iteration method, The above linear system was solved using the Gauss-Seidel iteration method. Although we were unable to theoretically prove the convergence of the Gauss-Seidel method for this system, numerical results indicate that, at each time level, convergence is typically achieved within a few iterative steps. To ensure the reliability of the iterative solution, we adopt the following stopping criteria:

$$\max\{|P^{n,k} - P^{n,k-1}|_{0,\infty}, |Q^{n,k} - Q^{n,k-1}|_{0,\infty}\} < \varrho = 10^{-8},$$
 when the above condition is met, it will be set $P^n \equiv P^{n,k}$, $Q^n \equiv Q^{n,k}$. (9)

NUMERICAL RESULTS 3.

ONE-DIMENSIONAL SIMULATION

The numerical simulation was conducted in one dimension with $\lambda = [0, L]$, for $0 \le t \le T$ with mesh points $x_i = jh$, $j = 0, \dots, J$ where h = L/J. The solution to the differential equation was calculated in the interval $\lambda = [0, L] = [0, 1]$ with h = 0.5, as well as the adoption of I = 10, if $\gamma = 0$, then the system with Neumann boundary conditions, and if $\gamma = 1$, then the system with Robin boundary conditions. Here, we adopt the following examples:

$$p(x,0) = 1 + 0.5x,$$
 $q(x,0) = 0.5.$ (10)

For $w_1 = -5$, $w_2 = 1$, and $\Delta t = 0.0001$, the numerical solution was calculated. Figures 1 and 2 show the numerical solution for the time level T = 10. These figures show that the solutions have a positive property and do not produce any negative values. It was established in [22] that the system is attracted to the equilibrium point (q^*, p^*) . If $\gamma = 0$, then we have Neumann boundary conditions; however, if $\gamma = 1$, then we have Robin boundary conditions. The solutions maintain positive and converge to the system's equilibrium point.

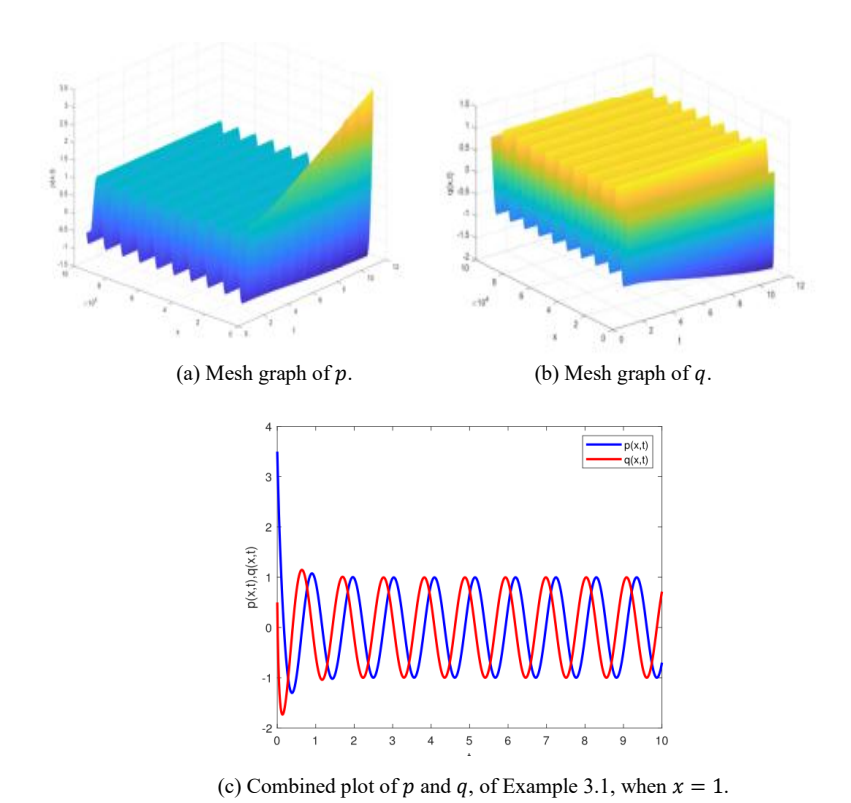


FIGURE 1. - Graphs for p and q at $w_1 = -5$, $w_2 = 1$, $\gamma = 0$, and $\Delta t = 0.0001$.

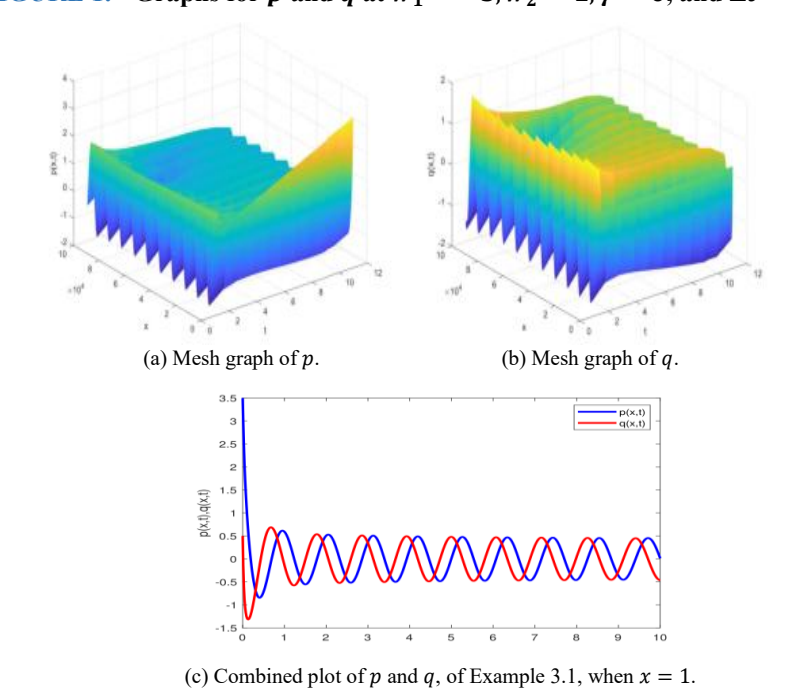


FIGURE 2. - Graphs for p and q at $w_1=-5, w_2=1, \gamma=1,$ and $\Delta t=0.0001.$

Example 3.2. The second example adopted the following:

$$p(x,0) = 0.01,$$
 $q(x,0) = 0.$ (11)

The constants used in the calculation of the numerical solutions are as follows: $w_1 = 3$, $w_2 = 2$, and $\Delta t = 0.0001$. Figures 3 and 4 present the numerical solution for this example at the specified time level. T = 10. It has been proven in [22] that the system's equilibrium point (q^*, p^*) is stable

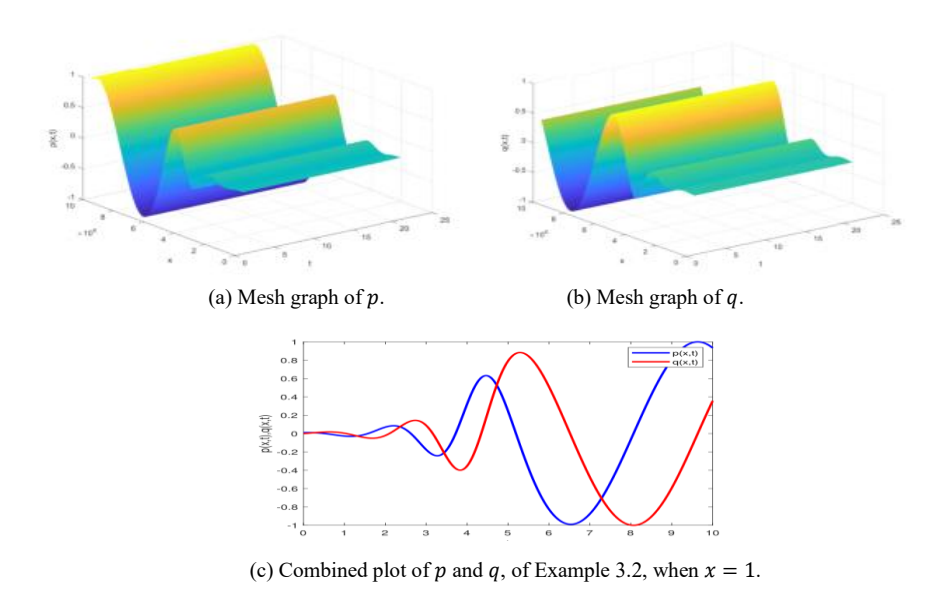


FIGURE 3. - Graphs for p and q at $w_1 = 3$, $w_2 = 2$, $\gamma = 0$, and $\Delta t = 0.0001$.

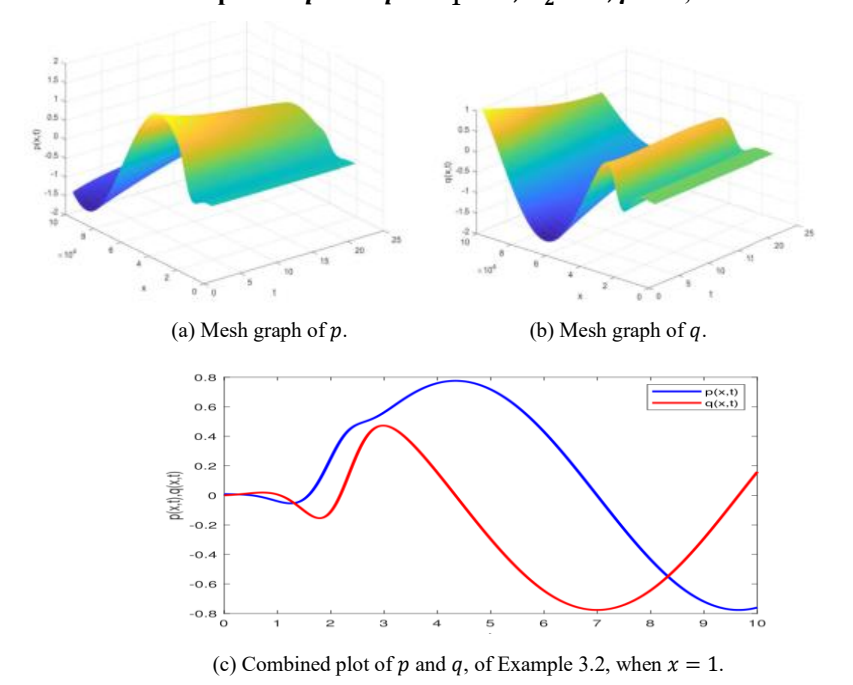


FIGURE 4. - Graphs for p and q at $w_1 = 3$, $w_2 = 2$, $\gamma = 1$, and $\Delta t = 0.0001$.

3.2. TWO-DIMENSIONAL SIMULATION

We used $\lambda = [0, L] \times [0, L]$ and a square uniform mesh with vertices $(x_i, y_j) = (ih, jh)$, where i, j = 0, ..., J. Note h = L/J, The same spatial step was used in both the xxx and yyy directions. A "right-angled" triangulation was employed, in which each square is divided by a diagonal running from the top-right corner to the bottom-left corner. The nodes were ordered in the "natural" manner: numbering from left to right, starting with the bottom row.

Example 3.3. In this example, the parameters are chosen such that T = 5, $w_1 = -5$, $w_2 = 1$, $\gamma = 1$, and the problem is solved over the domain $\lambda = [0,1] \times [0,1]$ with h = 0.05, $\Delta t = 0.001$ and J = 100. The initial conditions considered are:

$$p(x, y, 0) = 1 + 0.5x, \quad q(x, y, 0) = 0.5.$$
 (12)

The numerical solutions of p and q, for the time level T=5, are shown in Figures 5 and 6.

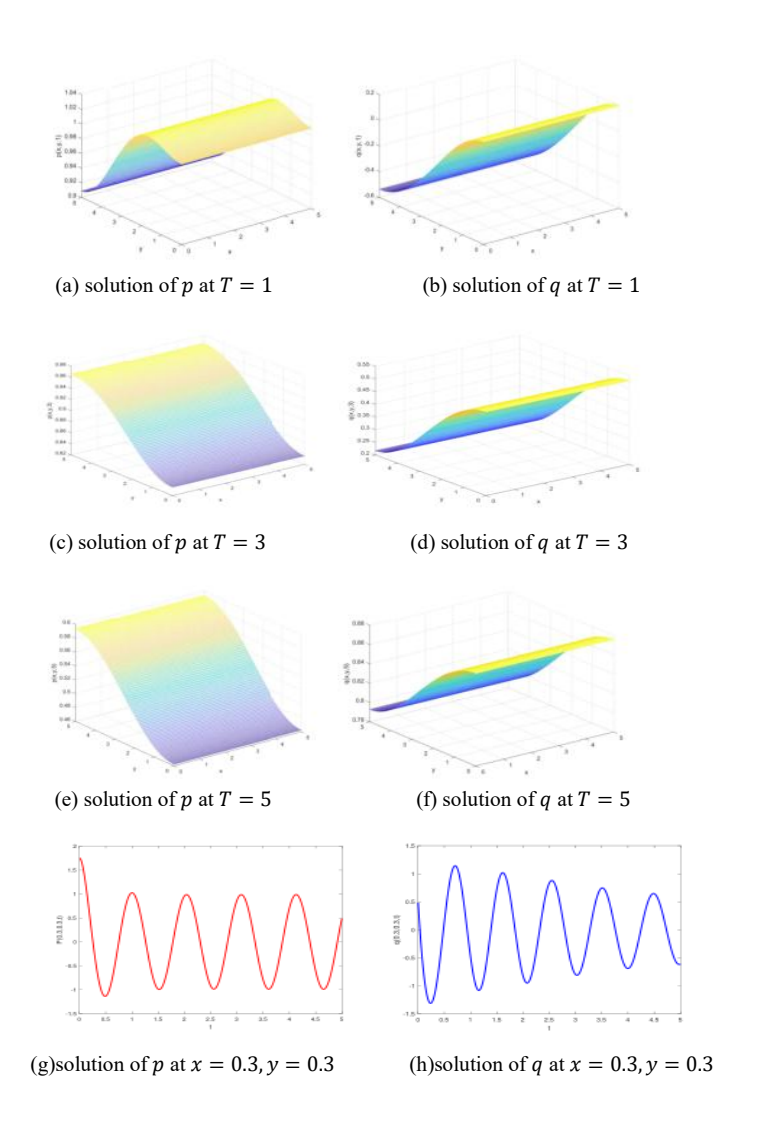
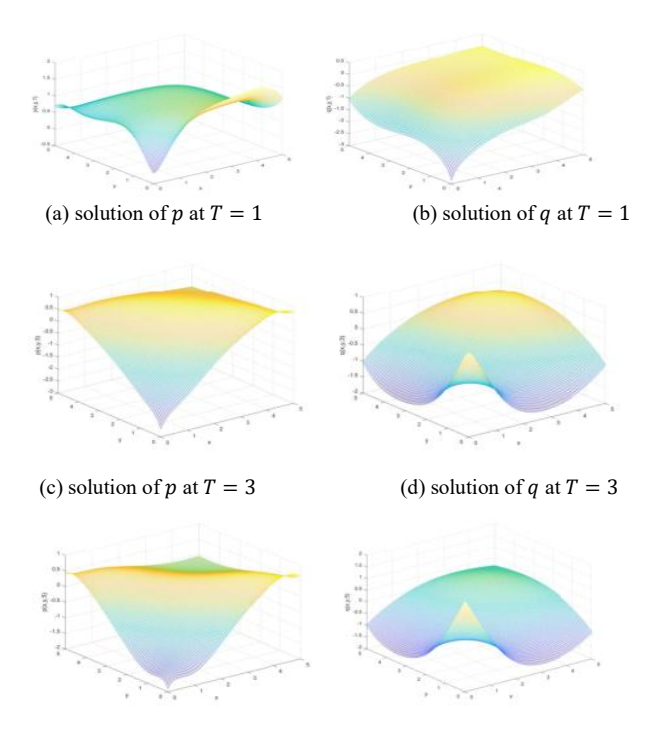


FIGURE 5. - Numerical solution of p, of Example 3.3, at $w_1 = -5$, $w_2 = 1$, $\gamma = 0$.



(e) solution of p at T = 5

(f) solution of q at T = 5

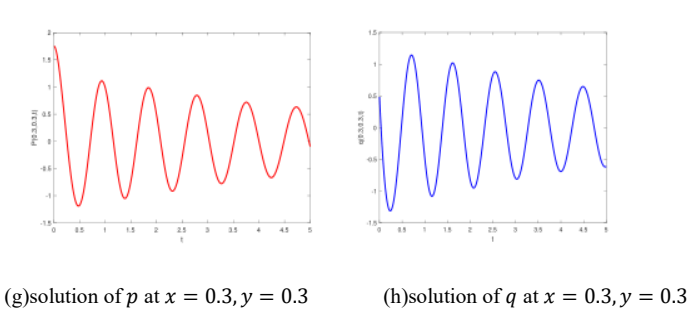


FIGURE 6. - Numerical solution of q, of Example 3.3, at $w_1 = -5$, $w_2 = 1$, $\gamma = 1$.

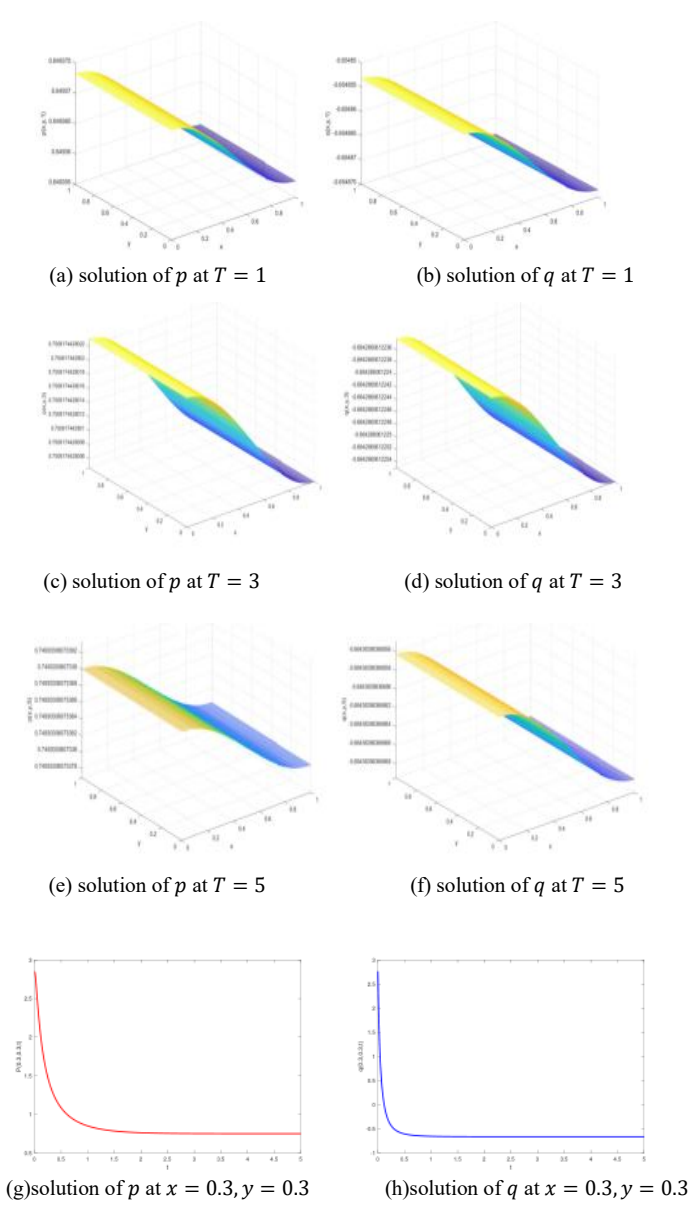


FIGURE 7. - Numerical solution of p , of Example 3.4, at $w_1=w_2=1, \gamma=0$.

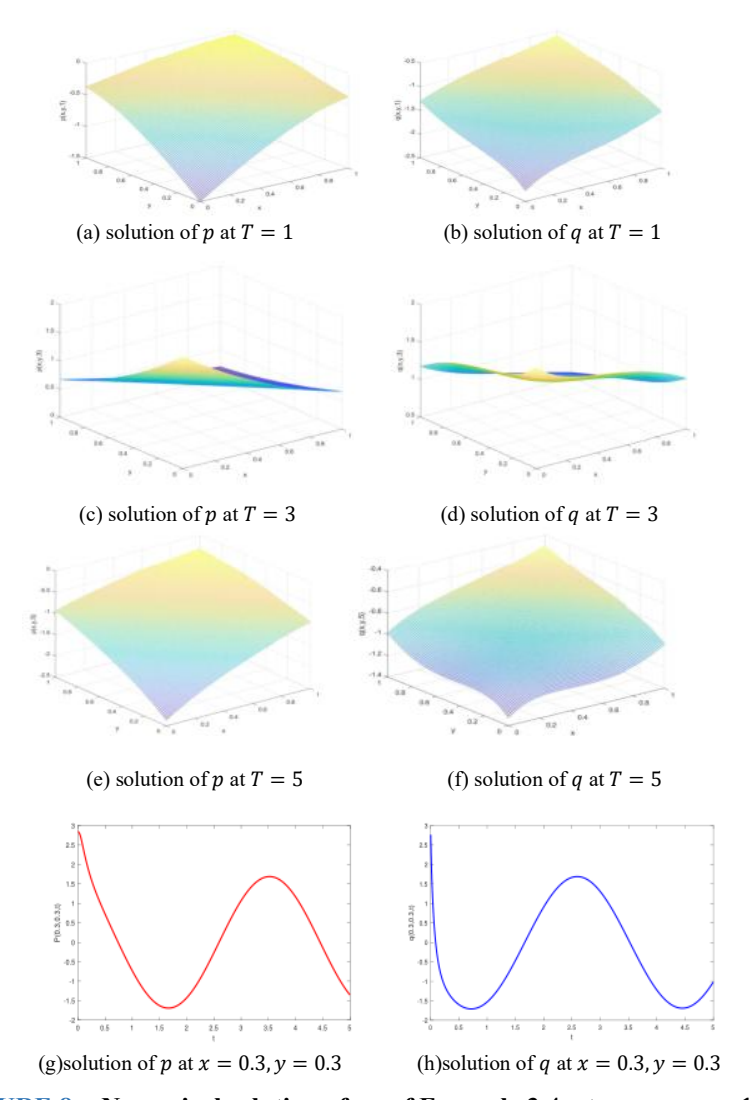
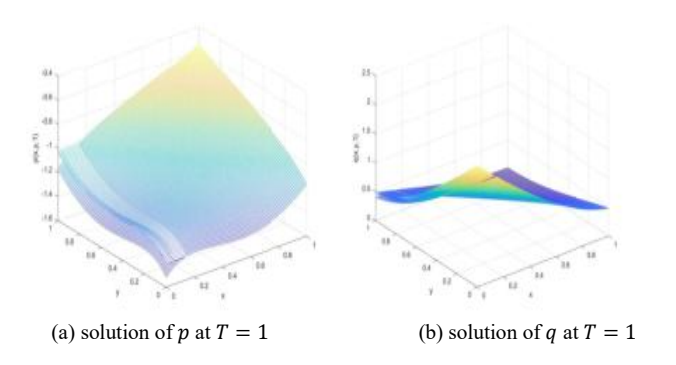


FIGURE 8. - Numerical solution of q , of Example 3.4, at $w_1=w_2=1$, $\gamma=1$.

Example 3.5. In this example, the parameters are chosen such that T = 5, $w_1 = 1$, $w_2 = 2$, $\gamma = 1$, and the problem is solved over the domain $\lambda = [0,1] \times [0,1]$ with h = 0.01, $\Delta t = 0.001$ and J = 100. The initial conditions considered are:

$$p(x, y, 0) = exp(1 + 0.2x), q(x, y, 0) = exp(2 + 0.5y).$$
 (14)

The numerical solutions of p and q, for the time level T=5, are shown in Figure 9.



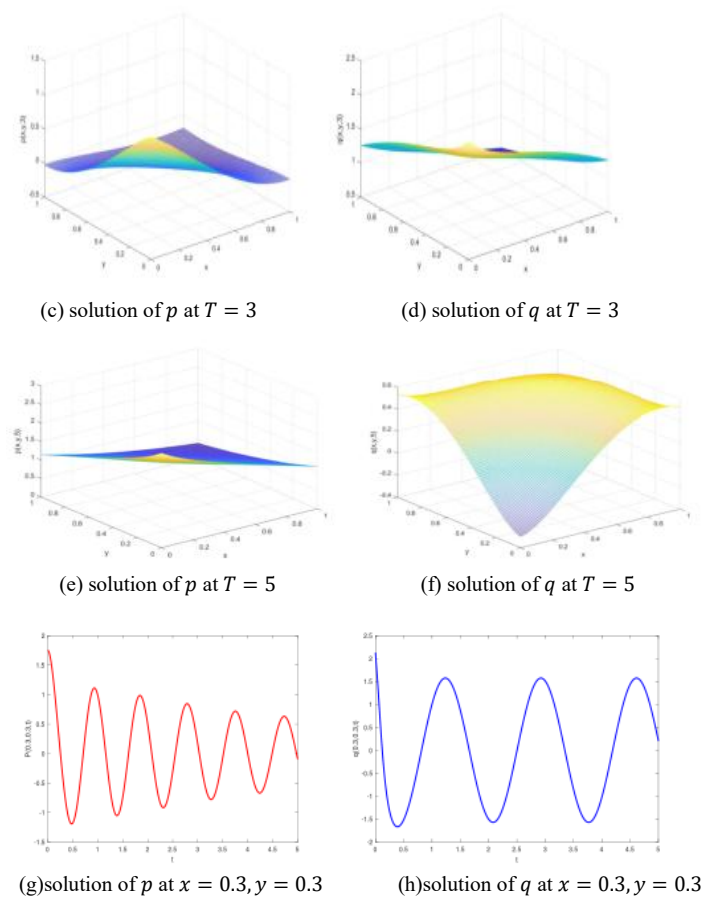


FIGURE 9. - Numerical solution of p, of Example 3.5, at $w_1 = 1$, $w_2 = 2$, $\gamma = 1$.

4. ERROR COMPUTATIONS

To evaluate the error, we make a simple modification to problem (H) by incorporating the source terms: $g_1(\mathbf{x}, t)$ and $g_2(\mathbf{x}, t)$, thus the systems (1)-(4) can be written in the form:

 (\widetilde{H}) Find $\{p, q\}$ such that

$$\frac{\partial p}{\partial t} = \Delta p + (1 - \rho^2)p - (\omega_1 - \omega_2 \rho^2)q + g_1(\mathbf{x}, t), \qquad \text{in} \qquad \lambda_T, \tag{15}$$

$$\frac{\partial q}{\partial t} = \Delta q + (\omega_1 - \omega_2 \rho^2) p + (1 - \rho^2) q + g_2(\mathbf{x}, t), \qquad \text{in} \qquad \lambda_T, \tag{16}$$

As a result, we consider the following modified approximation of the problem:

Find $\{P^n, Q^n\} \in S^h \times S^h$, such that for all $\varpi^h \in S^h$

$$\frac{(P^{n,k} - P^{n-1})^{n-1}}{\Delta t}, \varpi^{h})^{h} + (\nabla P^{n,k}, \nabla \varpi^{h}) + \gamma \int_{\partial \lambda} P^{n,k} \varpi^{h} dA$$

$$= ((1 - (\rho^{n,k-1})^{2})P^{n,k}, \varpi^{h})^{h} - ((w_{1} - w_{2}(\rho^{n,k-1})^{2})Q^{n,k-1}, \varpi^{h})^{h} + (g_{1}(\mathbf{x}, t), \varpi^{h})^{h}, \tag{17}$$

$$(\frac{Q^{n,k} - Q^{n-1}}{\Delta t}, \varpi^h)^h + (\nabla Q^{n,k}, \nabla \varpi^h) + \gamma \int_{\partial \lambda} Q^{n,k} \varpi^h dA = ((w_1 - w_2(\rho^{n,k-1})^2)P^{n,k-1}, \varpi^h)^h + ((1 - (\rho^{n,k-1})^2)Q^{n,k-1}, \varpi^h)^h + (g_2(\mathbf{x}, t), \varpi^h)^h.$$
(18)

4.1 ONE-DIMENSIONAL ERROR

Three numerical examples, which are solutions to the systems (15) and (16), are introduced. The first example satisfies Neumann boundary conditions $\gamma = 0$. In the other examples, we have introduced Robin boundary conditions

 $\gamma = 1$. For simplification, we used $w_1 = w_2 = 1$, $\lambda = [0,1]$, and T = 1 in all examples. From the associated exact solutions of each case, the source terms $g_1(x,t)$, $g_2(x,t)$ and can be derived. We divide the domain $\lambda = [0,1]$ into N uniform intervals and set the mesh size for each element to h = 1/N. The exact solution are as follows:

(i)
$$p = \exp(t + 3x),$$

$$q = \exp(2t + 2x),$$
 (ii)
$$p = 1 + \exp(2t)\cos(2\pi x),$$

$$q = 1 + \exp(-3t)\cos(\pi x),$$
 (iii)
$$p = 2 + \exp(-6t)\sin(4\pi y),$$

$$q = 2 + \exp(-4t)\sin(2\pi y),$$

The associated L^2 , L^∞ -Norms errors for a group of simulations are presented in Tables 1-3. The numerical results of the error demonstrate that as J increases, i.e, as the value of h decreases, the error's value reduces. Additionally, the error for $\Delta t = 0.00001$ is the same as for $\Delta t = 0.000001$, indicating that our numerical technique produces extremely accurate results for a variety of Δt values.

Table 1. - Discrete L^2 , L^{∞} -norms error for one-dimensional problem with homogeneous Neumann boundary condition of the Case (i).

	$\Delta t = 0.00001$				$\Delta t = 0.000001$				
	$\parallel p - P \parallel$		$\parallel q-Q \parallel$		$\parallel p - P \parallel$		$\parallel q-Q \parallel$		
h	L^2	L^{∞}	L^2	L^{∞}	L^2	L^{∞}	L^2	L^{∞}	
0.1	4.55E-04	4.20E-06	1.41E-04	1.18E-06	1.44E-04	4.20E-07	4.47E-05	1.18E-07	
0.05	5.64E-04	6.67E-06	1.27E-04	1.15E-06	1.10E-04	4.18E-07	4.00E-05	1.15E-07	
0.04	5.05E-04	5.47E-06	1.15E-04	1.15E-06	1.03E-04	3.48E-07	3.26E-05	1.11E-07	
0.025	3.63E-04	9.68E-07	1.00E-04	1.05E-06	8.42E-05	3.21E-07	2.38E-05	1.05E-07	
0.02	1.83E-04	1.01E-06	1.93E-05	4.59E-07	4.49E-05	1.00E-07	1.09E-05	1.00E-07	

Table 2. - Discrete L^2 , L^{∞} -norms error for one-dimensional problem with homogenous Robin boundary condition of the Case (ii).

	$\Delta t = 0.00001$				$\Delta t = 0.000001$				
	$\parallel p - P \parallel$		$\parallel q - Q \parallel$		$\parallel p - P \parallel$		$\parallel q-Q \parallel$		
h	L^2	L^{∞}	L^2	L^{∞}	L^2	L^{∞}	L^2	L^{∞}	
0.1	6.05E-02	3.95E-04	7.99E-02	4.43E-04	1.91E-02	3.95E-05	2.53E-02	4.43E-05	
0.05	5.42E-02	3.61E-04	7.22E-02	4.40E-04	2.03E-02	4.61E-05	2.60E-02	4.90E-05	
0.04	4.49E-02	3.15E-04	6.27E-02	4.00E-04	2.05E-02	4.75E-05	2.61E-02	5.00E-05	
0.025	1.60E-02	2.98E-04	6.14E-02	3.16E-04	2.09E-02	4.98E-05	2.64E-02	5.15E-05	
0.02	6.64E-03	1.06E-04	6.06E-02	1.21E-04	2.10E-02	5.06E-05	2.64E-02	5.21E-05	

Table 3. - Discrete L^2 , L^{∞} -norms error for one-dimensional problem with homogenous Robin boundary condition of the Case (iii).

	$\Delta t = 0.00001$				$\Delta t = 0.000001$				
	$\parallel p - P \parallel$		$\parallel q-Q \parallel$		$\parallel p - P \parallel$		$\parallel q-Q \parallel$		
h	L^2	L^{∞}	L^2	L^{∞}	L^2	L^{∞}	L^2	L^{∞}	
0.1	8.57E-04	5.08E-06	3.64E-04	1.99E-06	2.71E-04	5.08E-07	1.15E-04	1.99E-07	
0.05	8.48E-04	4.27E-06	2.60E-04	1.59E-06	2.00E-04	4.27E-07	1.14E-04	1.99E-07	
0.04	7.65E-04	4.13E-06	2.59E-04	1.40E-06	1.05E-04	3.53E-07	1.04E-04	1.50E-07	
0.025	5.90E-04	3.92E-06	1.59E-04	1.20E-06	7.13E-05	3.22E-07	6.13E-05	1.40E-07	
0.02	2.98E-04	2.06E-06	3.58E-05	1.10E-06	3.16E-05	2.06E-07	4.13E-05	9.99E-08	

4.2 TWO-DIMENSIONAL ERROR

In this section, we explore two numerical examples corresponding to systems (15) and (16), similar to the approach used in the one-dimensional case. In the first example, Neumann boundary conditions are applied. The second example also satisfies Neumann boundary conditions, which correspond to Robin boundary conditions with $\gamma=1$ gamma = $1\gamma=1$. The fourth example satisfies the Robin boundary conditions. For all cases, we used $w_1=w_2=1$, $\lambda=[0,1]\times[0,1]$, and T=1. The initial and boundary conditions, as well as the source terms $g_1(x,y,t), g_2(x,y,t), can be deduced from the exact solution of each case. The Exact solutions are in the following forms:$

(i)
$$p = 2 + exp(-2t)cos(3\pi x))cos(3\pi (x + y)).$$

$$q = 2 + exp(-2t)cos(2\pi x)cos(2\pi (x + y)),$$
 (ii)
$$p = exp(0.5t + x + y),$$

$$q = exp(0.5t + x^2 + y^2).$$

The associated L^2 , L^{∞} -norms error for a collection of simulations is provided in Tables 4 and 5. In the two-dimensional situation, the error behavior is identical to that of the one-dimensional case.

Table 4. - Discrete L^2 , L^{∞} -norms error for a two-dimensional problem with homogeneous Neumann boundary conditions of Case (i).

boundary conditions of case (i).										
	$\Delta t = 0.00001$				$\Delta t = 0.000001$					
	$\parallel p - P \parallel$		$\parallel q-Q \parallel$		$\parallel p - P \parallel$		$\parallel q-Q \parallel$			
h	L^2	L^{∞}	L^2	L^{∞}	L^2	L^{∞}	L^2	L^{∞}		
0.1	4.11E-07	1.23E-05	3.75E-07	1.09E-05	4.11E-08	1.23E-06	3.75E-08	1.09E-06		
0.05	2.80E-07	1.86E-05	2.45E-07	1.59E-05	2.80E-08	1.16E-06	2.45E-08	1.06E-06		
0.04	2.36E-07	1.79E-05	2.03E-07	1.67E-05	2.36E-08	1.09E-06	2.03E-08	1.06E-06		
0.025	1.57E-07	1.27E-05	1.33E-07	1.77E-05	1.57E-08	1.01E-06	1.33E-08	7.73E-07		
0.02	1.28E-07	1.21E-05	1.07E-07	1.51E-05	1.28E-08	1.01E-06	1.07E-08	6.10E-07		

Table 5. - Discrete L^2 , L^{∞} -norms error for a two-dimensional problem with a homogeneous Robin boundary condition of Case (ii).

	$\Delta t = 0.00001$				$\Delta t = 0.000001$				
	$\parallel p - P \parallel$		$\parallel q-Q \parallel$		$\parallel p - P \parallel$		$\parallel q-Q \parallel$		
h	L^2	L^{∞}	L^2	L^{∞}	L^2	L^{∞}	L^2	L^{∞}	
0.1	4.61E-06	1.34E-04	5.03E-06	1.33E-04	4.61E-07	1.34E-05	5.03E-07	1.33E-05	
0.05	2.71E-06	1.76E-04	2.51E-06	1.43E-04	2.71E-07	1.76E-05	2.51E-07	1.43E-05	
0.04	2.24E-06	1.75E-04	2.00E-06	1.43E-04	2.24E-07	1.85E-05	2.00E-07	1.44E-05	
0.025	1.46E-06	1.40E-04	1.24E-06	1.43E-04	1.46E-07	2.00E-05	1.24E-07	1.45E-05	
0.02	1.19E-06	1.21E-04	9.92E-07	1.05E-04	1.19E-07	2.01E-05	9.92E-08	1.45E-05	

5. CONCLUSIONS

In this paper, we derived numerical solutions for a nonlinear predator—prey system using the finite element method. Our primary objective was to analyze the system's dynamics while quantifying the error between the numerical and continuous solutions. The finite element method effectively captured the intricate behaviors of predator—prey interactions, producing numerical solutions that exhibited positive characteristics and indicated system stability. The results showed that decreasing the mesh size led to faster convergence of the numerical solutions toward the true solution.

To assess the accuracy of our approach, we conducted a thorough error analysis, providing estimates by comparing the numerical solutions with the continuous solutions. The findings revealed a significant reduction in error with increased mesh refinement, confirming the efficiency of the employed method. Tables illustrating errors across various test cases enabled a comprehensive evaluation of the method's performance.

Overall, our results reinforce the reliability of the numerical solutions and highlight the potential of this framework for more complex ecological models. This research contributes to a deeper understanding of predator—prey dynamics and establishes a foundation for developing effective computational strategies to study such intricate biological interactions.

REFERENCES

- [1] A. A. Al Ghafli and H. J. Al Salman, "An improved error bound for a finite element approximation of a reaction-diffusion system of λ ω type," Applied Mathematics and Computation, vol. 246, pp. 491–501, 2014.
- [2] G. A. Al-Juaifri and A. J. Harfash, "Analysis of a nonlinear reaction-diffusion system of the FitzHugh-Nagumo type with Robin boundary conditions," Ricerche di Matematica, vol. 72, no. 1, pp. 335–357, 2023.
- [3] A. M. Alqahtani, "Numerical simulation to study the pattern formation of reaction-diffusion Brusselator model arising in triple collision and enzymatic," Journal of Mathematical Chemistry, vol. 56, no. 6, pp. 1543–1566, 2018.
- [4] J. W. Barrett and J. F. Blowey, "An error bound for the finite element approximation of the Cahn-Hilliard equation with logarithmic free energy," Numerische Mathematik, vol. 72, no. 1, pp. 1–20, 1995.
- [5] J. W. Barrett and J. F. Blowey, "Finite element approximation of a nonlinear cross-diffusion population model," Numerische Mathematik, vol. 98, no. 2, pp. 195–221, 2004.
- [6] A. Borzì, "Solution of lambda-omega systems: Theta-schemes and multigrid methods," Numerische Mathematik, vol. 98, pp. 581–606, 2004.
- [7] N. F. Britton et al., Reaction-Diffusion Equations and Their Applications to Biology, Academic Press, 1986.
- [8] P. G. Ciarlet and P.-A. Raviart, "General Lagrange and Hermite interpolation in \mathbb{R}^n with applications to finite element methods," Archive for Rational Mechanics and Analysis, vol. 46, no. 3, pp. 177–199, 1972.
- [9] M. Dehghan and V. Mohammadi, "The boundary knot method for the solution of two-dimensional advection reaction-diffusion and Brusselator equations," International Journal of Numerical Methods for Heat & Fluid Flow, vol. 31, no. 1, pp. 106–133, 2020.
- [10] Z. Dong and H. Li, "A space-time finite element method based on local projection stabilization in space and discontinuous Galerkin method in time for convection-diffusion-reaction equations," Applied Mathematics and Computation, vol. 397, p. 125937, 2021.
- [11] M. H. Hashim and A. J. Harfash, "Finite element analysis of attraction-repulsion chemotaxis system. Part I: Space convergence," submitted for publication.
- [12] L. J. Khaled-Abad and R. Salehi, "Application of weak Galerkin finite element method for nonlinear chemotaxis and haptotaxis models," Applied Mathematics and Computation, vol. 409, p. 126436, 2021.
- [13] N. Kopell and L. N. Howard, "Plane wave solutions to reaction-diffusion equations," Studies in Applied Mathematics, vol. 52, no. 4, pp. 291–328, 1973.
- [14] D. Krause and R. Krause, "Enabling local time stepping in the parallel implicit solution of reaction-diffusion equations via space-time finite elements on shallow tree meshes," Applied Mathematics and Computation, vol. 277, pp. 164–179, 2016.
- [15] X. Li and W. Huang, "A study on nonnegativity preservation in finite element approximation of Nagumo-type nonlinear differential equations," Applied Mathematics and Computation, vol. 309, pp. 49–67, 2017.
- [16] Y. Li and M. Feng, "A local projection stabilization virtual element method for convection-diffusion-reaction equation," Applied Mathematics and Computation, vol. 411, p. 126536, 2021.
- [17] T. Lin and N. Madden, "A finite element analysis of a coupled system of singularly perturbed reaction-diffusion equations," Applied Mathematics and Computation, vol. 148, no. 3, pp. 869–880, 2004.

- [18] J. D. Murray, Mathematical Biology, 2nd ed., Springer-Verlag, Berlin, Heidelberg, New York, 1993.
- [19] S. Phongthanapanich and P. Dechaumphai, "Combined finite volume element method for singularly perturbed reaction-diffusion problems," Applied Mathematics and Computation, vol. 209, no. 2, pp. 177–185, 2009.
- [20] J. A. Sherratt, "A comparison of two numerical methods for oscillatory reaction-diffusion systems," Applied Mathematics Letters, vol. 10, no. 2, pp. 1–5, 1997.
- [21] J. A. Sherratt, "A comparison of periodic travelling wave generation by Robin and Dirichlet boundary conditions in oscillatory reaction–diffusion equations," IMA Journal of Applied Mathematics, vol. 73, no. 5, pp. 759–781, 2008.
- [22] E. Twizell, A. Gumel, and Q. Cao, "A second-order scheme for the Brusselator reaction-diffusion system," Journal of Mathematical Chemistry, vol. 26, no. 4, pp. 297–316, 1999.
- [23] A. I. Vol'pert, V. A. Volpert, and V. A. Volpert, Traveling Wave Solutions of Parabolic Systems, vol. 140, American Mathematical Society, 1994.
- [24] C. Xenophontos and L. Oberbroeckling, "A numerical study on the finite element solution of singularly perturbed systems of reaction-diffusion problems," Applied Mathematics and Computation, vol. 187, no. 2, pp. 1351–1367, 2007.
- [25] B. Zhang, S. Chen, and J. Zhao, "A posteriori error estimation based on conservative flux reconstruction for nonconforming finite element approximations to a singularly perturbed reaction-diffusion problem on anisotropic meshes," Applied Mathematics and Computation, vol. 232, pp. 1062–1075, 2014.
- [26] J. Zhang and X. Liu, "Convergence of a finite element method on a Bakhvalov-type mesh for singularly perturbed reaction-diffusion equation," Applied Mathematics and Computation, vol. 385, p. 125403, 2020.
- [27] J. Zhao, S. Chen, B. Zhang, and S. Mao, "Robust a posteriori error estimates for conforming and nonconforming finite element methods for convection-diffusion problems," Applied Mathematics and Computation, vol. 264, pp. 346–358, 2015.